Soft Matter

Dynamic Article Links

Cite this: *Soft Matter*, 2012, **8**, 8194

www.rsc.org/softmatter

PAPER

Swelling kinetics of polymer gels: comparison of linear and nonlinear theories†

Nikolaos Bouklas and Rui Huang*

Received 28th February 2012, Accepted 28th March 2012
DOI: 10.1039/c2sm25467k

The swelling of a polymer gel is a kinetic process coupling mass transport and mechanical deformation. Both linear and nonlinear theories have been used to describe the swelling kinetics. Here we present a comparison between a nonlinear theory for polymer gels and the classical theory of linear poroelasticity. We show that the two theories are consistent within the linear regime under the condition of small perturbation from an isotropically swollen state of the gel. The relationship between the material properties in the linear theory and those in the nonlinear theory is established by a linearization procedure. Both linear and nonlinear solutions are presented for swelling kinetics of substrate-constrained and freestanding hydrogel layers. Although the linear poroelasticity theory can be used to fit experimental data, it is cautioned that the applicability of the linear theory should be limited to relatively small swelling ratios. To remove the linear limitation, a new procedure is suggested to fit the experimental data with the nonlinear theory. Finally, we discuss the indentation experiment as an effective method for characterizing the mechanical and transport properties of polymer gels along with possible extensions of the method.

1. Introduction

A polymer gel swells significantly when imbibing a large amount of solvent (*e.g.*, water). Swelling is a kinetic process coupling mass transport and mechanical deformation, which depends on the interaction between the polymer network and the solvent. Both linear and nonlinear theories have been used to describe or predict the swelling kinetics of polymer gels under various conditions. Tanaka *et al.* derived a linear diffusion equation by treating the gel as a mixture of solid and liquid with a coefficient of friction for the interaction.[1,2] Alternatively, Scherer proposed a linear theory treating the gel as a continuum phase with the pore pressure (or solvent concentration) as a state variable.[3,4] The linear theory by Scherer is equivalent to the linear poroelasticity theory originally proposed by Biot[5] for soil consolidation. The two linear approaches have been compared,[6,7] and considerable differences noted.[7] Hui and Muralidharan[7] proposed an extension to the approach by Tanaka *et al.*, with which the two linear theories become identical. Recently, the theory of linear poroelasticity has been used extensively in combination with experimental measurements for characterizing the mechanical and transport properties of polymer gels.[8–15] In spite of remarkable success, it is well known that the linear theory is limited to relatively small deformation, while large deformation is common for polymer gels. In contrast, a variety of nonlinear approaches have been proposed for coupling large deformation and transport processes in polymer gels.[16–25] A comparison between the linear and nonlinear approaches would define the range of applicability for the linear theory. Moreover, a consistent nonlinear theory would extend the properties determined in the linear regime to the nonlinear regime, provided that the physical parameters in the nonlinear theory can be properly related to those in the linear theory.

In the current work we present a comparison between the nonlinear theory by Hong *et al.*[23] and the linear poroelasticity theory. We show that the two theories are consistent within the linear regime under the condition of small perturbation from an isotropically swollen state of the gel. As specific examples, we consider swelling kinetics of both substrate-constrained and freestanding hydrogel layers immersed in a solvent (Fig. 1). Although the linear poroelasticity theory can be used to fit the experimental data for both the constrained and free swelling kinetics,[11] it is cautioned that the applicability of the linear theory should be limited to relatively small swelling ratios. For large swelling ratios, we suggest a new procedure to fit the experimental data with the nonlinear theory. Finally, we discuss the indentation relaxation experiment as an effective method for characterizing the mechanical and transport properties of polymer gels within the linear regime but with possible extensions to the nonlinear regime.

Department of Aerospace Engineering and Engineering Mechanics, University of Texas at Austin, Austin, TX 78712, USA. E-mail: ruihuang@mail.utexas.edu; Tel: +1-512-471-7558

† Electronic supplementary information (ESI) available: Definition of linear elastic properties of gel; solution procedures for constrained and free swelling by the nonlinear and linear theories. See DOI: 10.1039/c2sm25467k

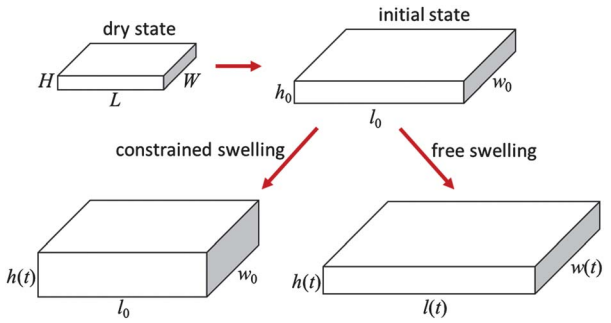

Fig. 1 Schematic illustration of a thin hydrogel layer, subject to constrained or free swelling. In the present study, the initial state is assumed to be isotropically swollen from the dry state with $h_0/H = l_0/L = w_0/W = \lambda_0$.

2. A nonlinear theory

Here we briefly summarize the nonlinear theory of polymer gels by Hong *et al.*[23] First, the constitutive behavior of a gel is described by using a free energy function. For a specific material model, the free energy density function based on the Flory–Rehner theory[26,27] takes the form

$$U(\mathbf{F}, C) = U_e(\mathbf{F}) + U_m(C) \tag{2.1}$$

$$U_e(\mathbf{F}) = \frac{1}{2}Nk_BT[F_{iK}F_{iK} - 3 - 2\ln(\det(\mathbf{F}))] \tag{2.2}$$

$$U_m(C) = \frac{k_BT}{\Omega}\left(\Omega C\ln\frac{\Omega C}{1+\Omega C} + \frac{\chi\Omega C}{1+\Omega C}\right) \tag{2.3}$$

where $F_{iJ} = \partial x_i/\partial X_J$ is the deformation gradient mapping the reference frame X_J to the current frame x_i, and C is the nominal solvent concentration (*i.e.*, number of solvent molecules per unit volume of polymer). Here, N is the effective number of polymer chains per unit volume of the polymer, χ is the Flory parameter for interaction between the solvent and the polymer, Ω is the volume per solvent molecule, T is the absolute temperature, and k_B is the Boltzmann constant.

Next assume that the volume of the gel changes only by solvent absorption/desorption so that

$$1 + \Omega C = \det(\mathbf{F}) \tag{2.4}$$

which imposes a constraint coupling deformation ($\mathbf{F}$) with the solvent concentration (C) in the gel. Eqn (2.4) implies that both the polymer network and solvent are incompressible. Using a Lagrange multiplier (Π), the free energy density function is re-written as

$$U(\mathbf{F}, C) = U_e(\mathbf{F}) + U_m(C) + \Pi[1 + \Omega C - \det(\mathbf{F})] \tag{2.5}$$

The chemical potential and the nominal stress in the gel are obtained as the thermodynamic work conjugates, namely

$$\mu = \frac{\partial U}{\partial C} = k_BT\left[\ln\frac{\Omega C}{1+\Omega C} + \frac{1}{1+\Omega C} + \frac{\chi}{(1+\Omega C)^2}\right] + \Omega\Pi \tag{2.6}$$

$$s_{iJ} = \frac{\partial U}{\partial F_{iJ}} = Nk_BT\left(F_{iJ} - \frac{1}{2}\left(\frac{1}{\det(\mathbf{F})} + \frac{\Pi}{Nk_BT}\right)e_{ijk}e_{JKL}F_{jK}F_{kL}\right) \tag{2.7}$$

where e_{ijk} is the alternating unit tensor.

In the absence of body forces, mechanical equilibrium of the gel requires

$$\frac{\partial s_{iJ}}{\partial X_J} = 0 \tag{2.8}$$

When the gel reaches a state of chemical equilibrium, the chemical potential is a constant everywhere. In the transient state, however, the gradient of the chemical potential drives solvent migration. By a diffusion model, the true flux of solvent at the current state is given as:[23]

$$j_k = -\frac{cD}{k_BT}\frac{\partial\mu}{\partial x_k} \tag{2.9}$$

where D is a constant for solvent diffusivity, c is the true solvent concentration which is related to the nominal concentration as $c = C/\det(\mathbf{F})$.

The nominal flux by definition is related to the true flux as: $J_KN_K\mathrm{d}S_0 = j_kn_k\mathrm{d}S$, where N_K and n_k are the unit normals in the reference and current frames, respectively. The differential areas, $\mathrm{d}S_0$ and $\mathrm{d}S$, are related as $F_{iK}n_i\mathrm{d}S = \det(\mathbf{F})N_K\mathrm{d}S_0$. Thus, by (2.9) the nominal flux is obtained as

$$J_K = \det(\mathbf{F})\frac{\partial X_K}{\partial x_k}j_k = -M_{KL}\frac{\partial\mu}{\partial X_L} \tag{2.10}$$

through which a nominal mobility tensor is defined as

$$M_{KL} = \frac{D}{\Omega k_BT}\left(\frac{\partial X_K}{\partial x_k}\frac{\partial X_L}{\partial x_k}\right)[\det(\mathbf{F}) - 1] \tag{2.11}$$

By conservation of solvent molecules, the evolution equation for the nominal solvent concentration is

$$\frac{\partial C}{\partial t} = -\frac{\partial J_K}{\partial X_K} = \frac{\partial}{\partial X_K}\left(M_{KL}\frac{\partial\mu}{\partial X_L}\right) \tag{2.12}$$

Therefore, a complete set of governing equations by the nonlinear theory includes the field equations in (2.8) and (2.12) along with the constitutive relations in (2.6), (2.7), and (2.10). In such a theory, the intrinsic material properties of the gel are specified by four independent quantities: N, χ, Ω, and D.

3. A linear theory

The theory of linear poroelasticity, originally developed by Biot[5] for soil consolidation, has been extended to gels.[3,4,6–15] In this section, by linearizing the equations of the nonlinear theory at the vicinity of an isotropically swollen state, we derive a set of linear equations for comparison with the theory of linear poroelasticity. With this, the relationship between the nonlinear and linear theories is established, and the material properties used in the linear theory are defined consistently based on the nonlinear theory.

The gel is assumed to be stress free and isotropically swollen at the initial state, with a swelling ratio λ_0 relative to the dry state in all directions. By setting $s_{iJ} = 0$ in (2.7), the Lagrange multiplier

Π is obtained, and by (2.6) the corresponding chemical potential for the initial state is

$$\frac{\mu_0}{k_B T} = \ln\frac{\lambda_0^3 - 1}{\lambda_0^3} + \frac{1}{\lambda_0^3} + \frac{\chi}{\lambda_0^6} + N\Omega\left(\frac{1}{\lambda_0} - \frac{1}{\lambda_0^3}\right) \tag{3.1}$$

Now consider a small perturbation to the initial state with a displacement field u_i. Relative to the initial state, a linear strain field is defined as

$$\varepsilon_{ij} = \frac{1}{2}\left(\frac{\partial u_i}{\partial x_j} + \frac{\partial u_j}{\partial x_i}\right) \tag{3.2}$$

By (2.4), the volumetric part of the strain is related to the change of solvent concentration, namely

$$\varepsilon_{kk} = \Omega(c - c_0) \tag{3.3}$$

where the concentration c is the number of solvent molecules per unit volume of the gel, and c_0 is the initial concentration that is related to the initial swelling ratio as $\Omega c_0 = 1 - \lambda_0^{-3}$.

Next we linearize the constitutive equations (2.6) and (2.7) at the vicinity of the initial state. For the chemical potential, we obtain that

$$\mu \approx \mu_0 + k_B T\left[\frac{1}{\lambda_0^3(\lambda_0^3 - 1)} - \frac{2\chi}{\lambda_0^6}\right]\varepsilon_{kk} + \Omega\delta\Pi \tag{3.4}$$

where $\delta\Pi$ is the perturbation of the Lagrange multiplier associated with the displacement field.

The Cauchy stress in the gel is related to the nominal stress as $\sigma_{ij} = s_{iK}F_{jK}/\det(\mathbf{F})$. After linearization, we obtain

$$\sigma_{ij} \approx \frac{2Nk_B T}{\lambda_0}\varepsilon_{ij} - (\Pi_0\varepsilon_{kk} + \delta\Pi)\delta_{ij} \tag{3.5}$$

where

$$\Pi_0 = Nk_B T\left(\frac{1}{\lambda_0} - \frac{1}{\lambda_0^3}\right) \tag{3.6}$$

Combining (3.4) and (3.5) to eliminate $\delta\Pi$, we obtain the Cauchy stress in the form

$$\sigma_{ij} = 2G\left[\varepsilon_{ij} + \frac{\nu}{1 - 2\nu}\varepsilon_{kk}\delta_{ij}\right] - \frac{\mu - \mu_0}{\Omega}\delta_{ij} \tag{3.7}$$

where

$$G = \frac{1}{\lambda_0}Nk_B T \tag{3.8}$$

$$\nu = \frac{1}{2} - \frac{N\Omega}{2}\left[\frac{1}{\lambda_0^2(\lambda_0^3 - 1)} + \frac{N\Omega}{\lambda_0^2} - \frac{2\chi}{\lambda_0^5}\right]^{-1} \tag{3.9}$$

As shown in Appendix A (ESI†), G and ν are the shear modulus and Poisson's ratio, respectively, of the isotropically swollen gel in the linear elastic regime; similar relations were obtained by Hu *et al.*[12]

Furthermore, linearizing the mechanical equilibrium equation in (2.8) leads to

$$\frac{\partial\sigma_{ij}}{\partial x_j} = 0 \tag{3.10}$$

By (2.9), the solvent flux at the vicinity of the initial state is approximately

$$j_k = -\frac{c_0 D}{k_B T}\frac{\partial\mu}{\partial x_k} = -M_0\frac{\partial\mu}{\partial x_k} \tag{3.11}$$

where

$$M_0 = \frac{D}{\Omega k_B T}\frac{\lambda_0^3 - 1}{\lambda_0^3} \tag{3.12}$$

By mass conservation, a linear evolution equation for the solvent concentration is obtained as

$$\frac{\partial c}{\partial t} = -\frac{\partial j_k}{\partial x_k} = M_0\frac{\partial^2\mu}{\partial x_k\partial x_k} \tag{3.13}$$

Therefore, based on the nonlinear theory, a complete set of linear equations can be developed, consisting of (3.10) and (3.13) for the field equations along with (3.7) and (3.11) as the constitutive relations. The linear kinematics is described by (3.2) and (3.3). Moreover, three material parameters for the linear equations are defined in (3.8), (3.9), and (3.12), which depend on the swelling ratio (λ_0) at the initial state.

In comparison with Biot's theory of linear poroelasticity, we note that the linear relation in (3.7) is identical to its counterpart in linear poroelasticity with the pore pressure, $p = (\mu - \mu_0)/\Omega$. Furthermore, Darcy's law in linear poroelasticity is equivalent to (3.11) by setting

$$M_0 = \frac{k}{\eta\Omega^2} \tag{3.14}$$

where k is the permeability of the polymer network and η is the viscosity of the solvent. All the other equations then become identical to Biot's theory. Therefore, the linear poroelasticity theory may be considered as a specialization of the nonlinear theory in the linear regime. In addition to the linear elastic shear modulus and Poisson's ratio in (3.8) and (3.9), the linear poroelastic property, k/η, is related to the intrinsic diffusivity D and the swelling ratio λ_0 by (3.14) and (3.12).

The linear equations can be further reduced by inserting (3.7) into (3.10):

$$G\left[\frac{\partial^2 u_i}{\partial x_j\partial x_j} + \frac{1}{1 - 2\nu}\frac{\partial^2 u_j}{\partial x_j\partial x_i}\right] = \frac{1}{\Omega}\frac{\partial\mu}{\partial x_i} \tag{3.15}$$

Next inserting (3.15) into (3.13), we obtain that

$$\frac{\partial c}{\partial t} = D^*\frac{\partial^2 c}{\partial x_j\partial x_j} \tag{3.16}$$

which takes the form of a linear diffusion equation in terms of the solvent concentration, with an effective diffusivity

$$D^* = \frac{2(1 - \nu)\Omega^2 GM_0}{1 - 2\nu} \tag{3.17}$$

Note that the effective diffusivity defined in (3.17) differs from the intrinsic diffusivity introduced in (2.9) for the nonlinear theory. The effective diffusivity (also called the cooperative diffusion coefficient[8]) is a combined quantity that depends on the initial state for the development of the linear theory.

4. Swelling of hydrogel layers

In this section we consider swelling kinetics in two cases (Fig. 1), one for a hydrogel layer laterally constrained by a rigid substrate and the other for a freestanding hydrogel layer immersed in a solvent. In both cases, we assume that the lateral dimensions of the hydrogel layer are much larger than the thickness (L, $W \gg H$) and hence ignore the edge effects. In each of the two cases we solve the transient problem based on the nonlinear theory and compare with the corresponding solution based on the linear theory. The detailed solution procedure is presented in Appendix B (ESI†), and the main results are discussed here.

4.1. Constrained swelling

Consider a layer of hydrogel with one face ($X = 0$) attached to a rigid substrate and the other face ($X = H$) exposed to a solvent, where H is the layer thickness in the dry state. Initially the gel is swollen isotropically with a swelling ratio λ_0. As more solvent molecules migrate into the gel, the gel swells in the direction of the thickness while the lateral dimensions are fixed by the substrate. Therefore, the stretch in the thickness direction is a function of time and position, $\lambda_2 = \lambda_2(X_2, t)$, whereas $\lambda_1 = \lambda_3 = \lambda_0$. By the nonlinear theory, the thickness swelling ratio can be obtained by solving a nonlinear diffusion equation

$$\lambda_0^2 \frac{\partial \lambda_2}{\partial t} = D \frac{\partial}{\partial X_2}\left(\xi \frac{\partial \lambda_2}{\partial X_2}\right) \tag{4.1}$$

where

$$\xi(\lambda_2) = \frac{1}{\lambda_0^2 \lambda_2^4} - \frac{2\chi\left(\lambda_0^2\lambda_2 - 1\right)}{\lambda_0^4 \lambda_2^5} + N\Omega \frac{\left(\lambda_0^2\lambda_2 - 1\right)\left(\lambda_2^2 + 1\right)}{\lambda_0^2 \lambda_2^4} \tag{4.2}$$

Eqn (4.1) is to be solved with the initial condition, $\lambda_2(t = 0) = \lambda_0$, and the boundary conditions including: (i) $s_{22}(X_2 = H) = 0$; (ii) $\mu(X_2 = H) = 0$; and (iii) $J_2(X_2 = 0) = 0$. The first two boundary conditions together require an instantaneous equilibrium swelling ratio at the upper surface, $\lambda_2(X_2 = H) = \lambda_\infty^c$, which can be obtained by solving a nonlinear algebraic equation

$$\ln\left(\frac{\lambda_0^2\lambda_\infty^c - 1}{\lambda_0^2\lambda_\infty^c}\right) + \frac{1}{\lambda_0^2\lambda_\infty^c} + \frac{\chi}{\lambda_0^4\left(\lambda_\infty^c\right)^2} + \frac{N\Omega}{\lambda_0^2}\left(\lambda_\infty^c - \frac{1}{\lambda_\infty^c}\right) = 0 \tag{4.3}$$

The zero flux condition at the lower surface requires that

$$\left(\frac{\partial \lambda_2}{\partial X_2}\right)_{X_2=0} = 0 \tag{4.4}$$

With the boundary conditions (4.3) and (4.4), a finite difference method is used to numerically integrate the nonlinear diffusion equation (4.1) (Appendix B, ESI†). Fig. 2a shows the numerical results, with λ_2 as a function of X_2 for increasing time, where the time is normalized by the characteristic time scale of diffusion, $\tau_1 = H^2/D$. Apparently, a sharp gradient of the swelling ratio develops near the upper surface at the early stage of swelling. Correspondingly, the solvent concentration, $C = (\lambda_0^2\lambda_2 - 1)/\Omega$, and the swelling-induced compressive stress are both inhomogeneous at the transient state. In particular, the compressive stress as shown in Fig. 2b may cause surface instability of the gel to form wrinkles and creases as observed experimentally.[28,29] For the present study we assume the surface

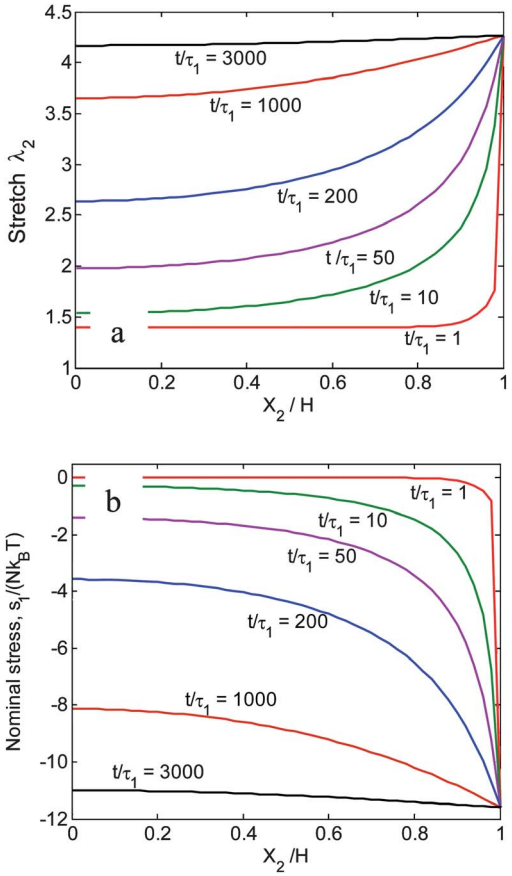

Fig. 2 Evolution of (a) stretch and (b) swelling induced compressive stress in a constrained hydrogel layer by the nonlinear theory, with $N\Omega = 0.001$, $\chi = 0.4$, and $\lambda_0 = 1.4$. The time is normalized by $\tau_1 = H^2/D$.

to remain flat during swelling. After a long time ($t \to \infty$), the hydrogel approaches the homogeneous equilibrium state with $\lambda_2 = \lambda_\infty^c$ everywhere. By (4.3), the equilibrium swelling ratio depends on the initial swelling ratio (λ_0) as well as two dimensionless parameters, $N\Omega$ and χ.

With the transient swelling ratio $\lambda_2(X_2, t)$, the thickness of the hydrogel layer can be calculated as

$$h(t) = \int_0^H \lambda_2(X_2, t)\mathrm{d}X_2 \tag{4.5}$$

Fig. 3a plots the relative thickness swelling ratio, $h(t)/h_0$, as a function of time for different values of χ, with initial thickness $h_0 = \lambda_0 H$. In all cases, the thickness increases rapidly at the early stage and eventually approaches the equilibrium state with $h_\infty/h_0 = \lambda_\infty^c/\lambda_0$. As the equilibrium swelling ratio increases with decreasing χ, the time to reach the equilibrium state increases.

At the limit of short time ($t \to 0$), the diffusion equation (4.1) can be linearized, yielding a self-similar solution, namely

$$\frac{\lambda_2 - \lambda_0}{\lambda_\infty^c - \lambda_0} = erfc\left(\frac{\lambda_0(H - X_2)}{2\sqrt{\xi(\lambda_0)Dt}}\right) \tag{4.6}$$

The change in thickness of the hydrogel layer is then obtained as

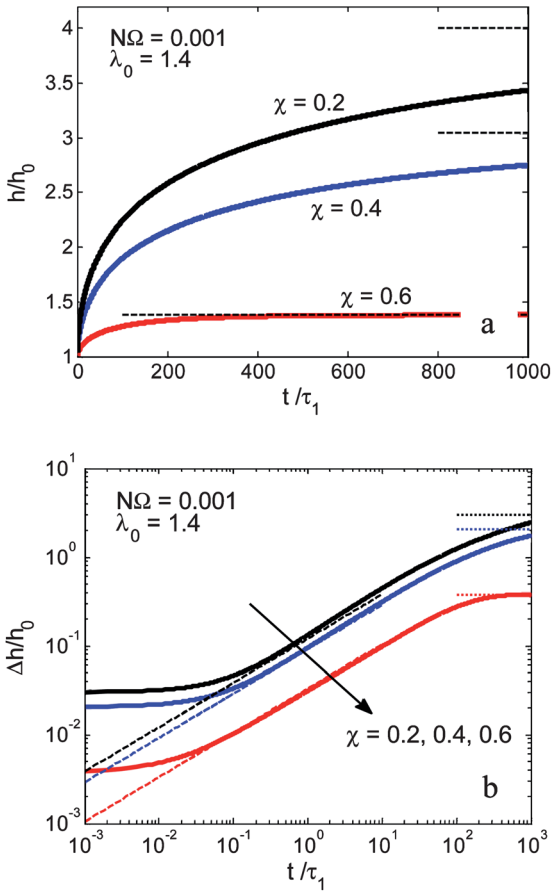

Fig. 3 (a) Thickness swelling ratio as a function of time for constrained hydrogel layers with $N\Omega = 0.001$, $\lambda_0 = 1.4$, and different values of χ. The horizontal dashed lines indicate the equilibrium swelling ratio, $h_\infty/h_0 = \lambda^c_\infty/\lambda_0$. (b) Normalized thickness change as a function of time, in comparison with the self-similar solution (dashed lines).

$$\Delta h(t) = \int_{-\infty}^{H} (\lambda_2 - \lambda_0)\mathrm{d}X_2 = 2\left(\frac{\lambda^c_\infty}{\lambda_0} - 1\right)\sqrt{\frac{\xi(\lambda_0)Dt}{\pi}} \tag{4.7}$$

As shown in Fig. 3b, the thickness change obtained numerically by the finite difference method scales with $\sqrt{t}$ in a window, roughly $0.1 < t/\tau_1 < 10$. The accuracy of the numerical method is limited by the spatial step ΔX. To reduce the numerical error in the early stage ($t/\tau_1 < 0.1$), we may reduce ΔX, which however would require a smaller time step Δt and thus higher computational cost for the numerical method to be stable. Alternatively, an unconditionally stable implicit method may be used to improve the numerical solution. It is found that the self-similar solution (4.7) tends to overestimate the swelling rate in the window $0.1 < t/\tau_1 < 10$ due to the use of $\xi(\lambda_0)$. As shown in Fig. 2a, the swelling ratio λ_2 is sharply graded between λ_0 and λ^c_∞ near the surface during the early stage of swelling. By taking $\xi = \xi(\lambda_0/2 + \lambda^c_\infty/2)$ in (4.7), the self-similar solution agrees closely with the numerical solution for $0.1 < t/\tau_1 < 10$ as shown in Fig. 3b.

The same problem of constrained swelling was solved by using the linear poroelasticity theory,[11,30,31] which predicts the thickness change of the hydrogel layer as

$$\Delta h(t) = \frac{(1-2\nu)(\hat{\mu}-\mu_0)h_0}{2(1-\nu)G\Omega} \times\left\{1 - \frac{8}{\pi^2}\sum_{n=0}^{\infty}\frac{1}{(2n+1)^2}\exp\left[-(2n+1)^2\frac{\pi^2 t}{4\tau_2}\right]\right\} \tag{4.8}$$

where $\tau_2 = h_0^2/D^*$ defines a time scale for the linear theory and $\hat{\mu}$ is the chemical potential of the solvent in the environment. After a long time ($t \to \infty$), the gel reaches the equilibrium with $\mu = \hat{\mu}$, and the equilibrium thickness change is

$$\Delta^c_\infty = \frac{(1-2\nu)(\hat{\mu}-\mu_0)h_0}{2(1-\nu)G\Omega} \tag{4.9}$$

At the limit of short time ($t/\tau_2 \ll 1$), a self-similar solution predicts that[11]

$$\Delta h(t) = \frac{2\Delta^c_\infty}{h_0}\sqrt{\frac{D^* t}{\pi}} \tag{4.10}$$

The results by the nonlinear and linear theories will be compared in Section 5.

4.2. Free swelling

Without the substrate constraint, solvent molecules enter the gel layer from both upper and lower surfaces, and the gel swells in both the thickness and in-plane directions. Again, we neglect the edge effects so that the solvent molecules migrate in the thickness direction only. By symmetry, the layer remains flat (no bending), with $\lambda_2 = \lambda_2(X_2, t)$ and $\lambda_1 = \lambda_3 = \lambda_1(t)$; the stretch in the in-plane direction is a function of time only. Based on the nonlinear theory, we obtain that

$$\lambda_1^2\frac{\partial\lambda_2}{\partial t} + 2\lambda_1\lambda_2\frac{\mathrm{d}\lambda_1}{\mathrm{d}t} = D\frac{\partial}{\partial X_2}\left(\bar{\xi}\frac{\partial\lambda_2}{\partial X_2}\right) \tag{4.11}$$

where

$$\bar{\xi}(\lambda_1,\lambda_2) = \frac{1}{\lambda_1^2\lambda_2^4} - \frac{2\chi(\lambda_1^2\lambda_2 - 1)}{\lambda_1^4\lambda_2^5} + N\Omega\frac{(\lambda_1^2\lambda_2 - 1)(\lambda_2^2 + 1)}{\lambda_1^2\lambda_2^4} \tag{4.12}$$

Furthermore, with no constraint, the in-plane stress must be self-balanced, namely

$$\int_0^H s_{11}\mathrm{d}X_2 = 0 \tag{4.13}$$

which leads to

$$\lambda_1^2 = \frac{1}{H}\int_0^H \lambda_2^2\mathrm{d}X_2 \tag{4.14}$$

Thus, the in-plane swelling ratio equals the root-mean-square (RMS) average of the out-of-plane swelling ratio.

The two nonlinear equations (4.11) and (4.14) can be solved simultaneously using a numerical method (Appendix B, ESI†), with the initial and boundary conditions: (i) $\lambda_2(t=0) = \lambda_1(t=0) = \lambda_0$; (ii) $s_{22}(X_2 = 0, H) = 0$; and (iii) $\mu(X_2 = 0, H) = 0$. The boundary conditions require that the swelling ratios at the surfaces ($X_2 = 0$ and H) satisfy

$$\ln\left(\frac{\lambda_1^2\lambda_2 - 1}{\lambda_1^2\lambda_2}\right) + \frac{1}{\lambda_1^2\lambda_2} + \frac{\chi}{\lambda_1^4\lambda_2^2} + \frac{N\Omega}{\lambda_1^2}\left(\lambda_2 - \frac{1}{\lambda_2}\right) = 0 \quad (4.15)$$

Unlike constrained swelling, however, the swelling ratio λ_2 at the surface is not a constant value for free swelling. Instead, it depends on λ_1 and is a function of time. Fig. 4 shows the numerical results, with λ_2 as a function of X_2 for increasing time in (a) and λ_1 as a function of time in (b). By (4.5), the thickness of the hydrogel layer is calculated as a function of time, which is also plotted in Fig. 4b. Apparently, the thickness swelling ratio, $h(t)/H$, follows closely with $\lambda_1(t)$, but not exactly, as expected from (4.14). Experimentally, the difference was found to be small, indistinguishable within the experimental uncertainty.[11,32] In Fig. 4c, the nominal in-plane stress (s_{11}) is plotted as a function of X_2 for increasing time. Due to the inhomogeneous swelling ratio at the transient state, the stress is compressive near the surfaces but tensile near the center, with zero resultant force. After a long time ($t \to \infty$), the gel approaches the homogeneous equilibrium state, with an isotropic swelling ratio and zero in-plane stress. The equilibrium swelling ratio can be obtained by solving eqn (4.15) with $\lambda_2 = \lambda_1 = \lambda^f_\infty$.

By the linear poroelasticity theory, the kinetic equation for free swelling of a hydrogel layer becomes[11]

$$\frac{\partial \mu}{\partial t} + 4G\Omega\frac{d\varepsilon_{11}}{dt} = D^*\frac{\partial^2 \mu}{\partial x_2^2} \quad (4.16)$$

In addition, by setting $\sigma_{22} = 0$, we obtain

$$2G\left(\frac{1-\nu}{1-2\nu}\right)\frac{\partial u_2}{\partial x_2} + 4G\left(\frac{\nu}{1-2\nu}\right)\varepsilon_{11} = \frac{\mu - \mu_0}{\Omega} \quad (4.17)$$

By requiring a vanishing resultant force in the in-plane direction, the in-plane strain is obtained as

$$\varepsilon_{11}(t) = \frac{u_2(h_0, t) - u_2(0, t)}{h_0} \quad (4.18)$$

A numerical method is used to solve (4.16)–(4.18) for the transient kinetics of free swelling (Appendix B, ESI†). In particular, no self-similar solution is found at the early stage of free swelling, and the thickness change at equilibrium ($t \to \infty$) can be obtained from (4.17) and (4.18) by setting $\mu = \hat{\mu}$:

$$\Delta^f_\infty = \frac{(1-2\nu)(\hat{\mu} - \mu_0)h_0}{2(1+\nu)G\Omega} \quad (4.19)$$

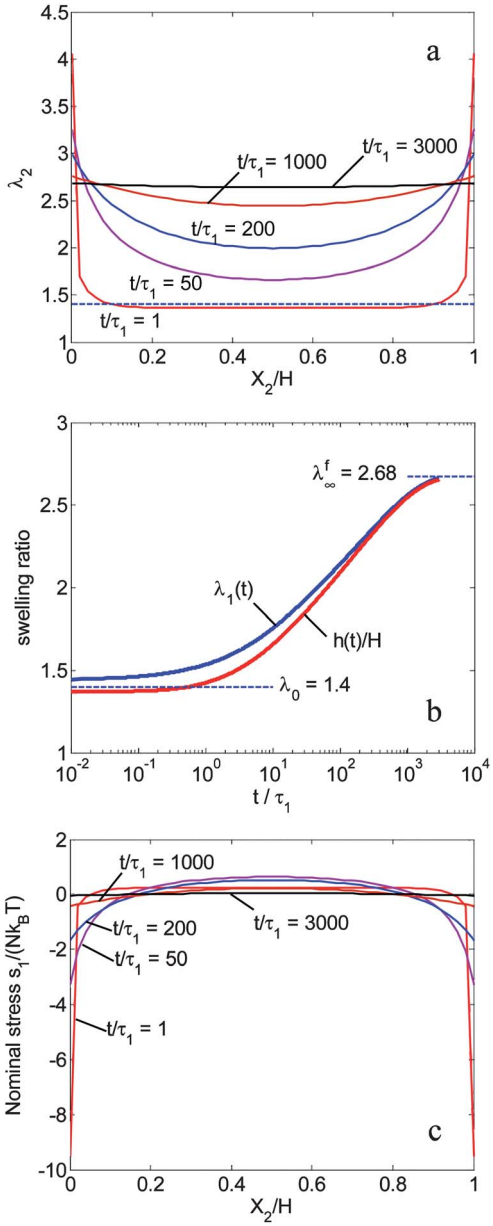

Fig. 4 Numerical results for free swelling of a hydrogel layer by the nonlinear theory ($\chi = 0.4$, $N\Omega = 0.001$, $\lambda_0 = 1.4$): (a) swelling ratio in the thickness direction; (b) in-plane swelling ratio (λ_1) and the average thickness ratio (h/H); (c) nominal stress in the in-plane direction.

5. Results and discussions

5.1. Linear poroelastic properties of gels

Under the condition of small deformation, the mechanical behaviour of a gel can be described by the theory of linear poroelasticity.[3–15] The physical parameters used in the linear theory, including the shear modulus (G), Poisson's ratio (ν), and permeability (k), are generally not intrinsic properties of the gel. Instead, they depend on the current state of the gel. On the other hand, the physical parameters in the nonlinear theory (N, χ, Ω, and D) are based on a microscopic model[26,27] and thus may be considered as intrinsic properties. For example, the shear modulus of a gel as defined in (3.8) depends on the initial swelling ratio λ_0 in addition to the polymer network, which has an initial shear modulus Nk_BT in the dry state. Since the swelling ratio depends on the chemical potential, as predicted in (3.1) by the nonlinear theory, the shear modulus of the gel, which may be measured by shear rheology, depends on the chemical potential of the environment. At the equilibrium chemical potential ($\mu = 0$), the shear modulus depends on the equilibrium swelling ratio, which in turn depends on the intrinsic parameters (χ and $N\Omega$). Similarly, Poisson's ratio as defined in (3.9) also depends on the initial swelling ratio (λ_0) as well as the intrinsic properties, as shown in Fig. 5a. Since the polymer network is assumed to be incompressible, the Poisson's ratio is 0.5 in the dry state ($\lambda_0 = 1$).

As the swelling ratio increases, the Poisson's ratio decreases; the gel becomes compressible due to solvent absorption/desorption. For each gel with specific intrinsic properties (χ and $N\Omega$), the Poisson's ratio at the equilibrium swelling ratio corresponding to $\mu = 0$ is plotted in Fig. 5b as a function of χ for different values of $N\Omega$. Interestingly, a sharp transition of the equilibrium Poisson's ratio is observed at $\chi \approx 0.5$, especially for gels with relatively small $N\Omega$. Thus, the Poisson's ratio of a gel is closely related to the intrinsic interaction between the polymer and the solvent. With a good solvent ($\chi < 0.5$), the swelling ratio is high, and the gel is highly compressible ($\nu = 0.2$ to 0.25) at the equilibrium swollen state.

By linear poroelasticity, the swelling kinetics depends on the ratio between permeability (k) and viscosity (η). By (3.12) and (3.14), we obtain that

$$\frac{k}{\eta} = \frac{\Omega D}{k_B T} \frac{\lambda_0^3 - 1}{\lambda_0^3} \tag{5.1}$$

Assuming a constant viscosity for the solvent, the permeability of the gel depends on the intrinsic diffusivity D as well as the swelling ratio λ_0. The permeability is zero in the dry state ($\lambda_0 = 1$) and increases with increasing swelling ratio. Intuitively, it may be understood that the permeability increases as a result of an increasingly open polymer network due to swelling.

It is noted here that the classical theory of linear poroelasticity assumes an isotropic behavior.[5] Taking an isotropically swollen state as the initial state, we recover the classical theory by linearizing the nonlinear theory. In general, however, the initial state is not necessarily isotropic. When swelling is constrained in one or two directions, the gel swells anisotropically.[33] The constrained swelling of a hydrogel layer on a rigid substrate is a common example. With an anisotropic initial state, linearization of the nonlinear theory would lead to a set of linear equations for anisotropic poroelasticity. Theories of anisotropic poroelasticity have been developed for geomaterials[34–37] and biomaterials (*e.g.*, bones),[38,39] while few studies have considered poroelastic anisotropy in gels.

5.2. Linear *vs.* nonlinear analysis of swelling

In Section 4, we present the analysis for constrained and free swelling of a hydrogel layer based on the nonlinear theory and the linear poroelasticity theory. For comparison, we plot in Fig. 6 the thickness ratio as a function of time for the constrained swelling, where the thickness is normalized by the initial thickness h_0 and the time is normalized by the time scale τ_1. By eqn (3.8), (3.12), and (3.17), the time scale for linear poroelasticity, τ_2, is converted to τ_1 as

$$\tau_2 = \tau_1 \frac{(1-2\nu)\lambda_0^6}{2(1-\nu)(\lambda_0^3 - 1)N\Omega} \tag{5.2}$$

For a specific gel with the intrinsic properties (χ and $N\Omega$), the swelling kinetics depends on the initial swelling ratio λ_0, governed by eqn (4.1) according to the nonlinear theory. On the other hand, the solution based on linear poroelasticity, as given in eqn (4.8), depends on the initial chemical potential (μ_0), which can be determined by (3.1). In addition, all the linear poroelastic properties, including G, ν, and the time scale τ_2, depend on the initial swelling ratio. As seen in Fig. 6, the linear theory agrees with the nonlinear theory at the early stage of swelling, both predicting a self-similar swelling with $\Delta h \propto \sqrt{t}$, which is expected following the linearization procedure in Section 3. However, the equilibrium thickness change ($\Delta_\infty^c = h_\infty - h_0$) predicted by the linear theory, as given in eqn (4.9), underestimates the equilibrium swelling in comparison with the nonlinear theory, as shown

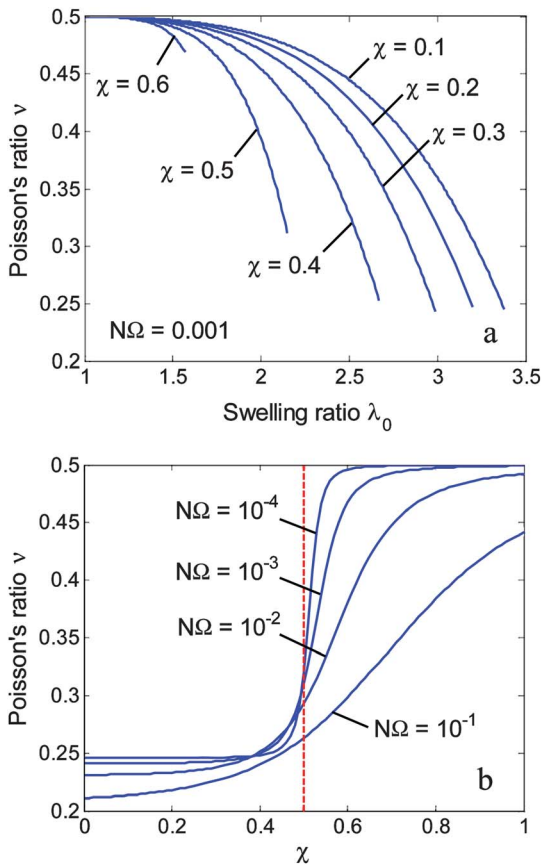

Fig. 5 (a) Poisson's ratio of polymer gels, as a function of the initial swelling ratio; (b) Poisson's ratio at the equilibrium swelling ratio as a function of χ.

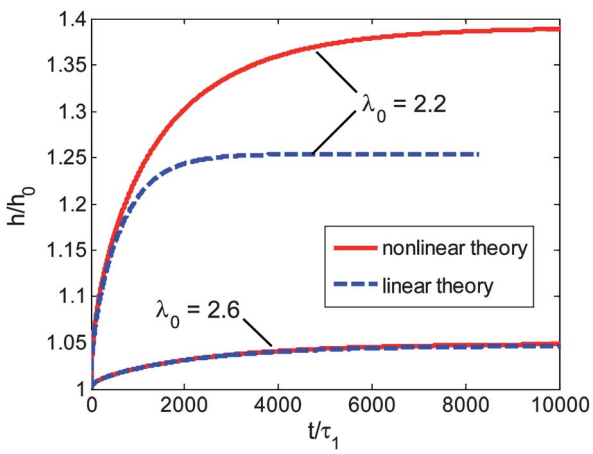

Fig. 6 Comparison between the nonlinear theory and the linear poroelasticity for constrained swelling of a hydrogel layer ($\chi = 0.4$ and $N\Omega = 0.001$).

in Fig. 7. The discrepancy is significant when the relative swelling ratio, h_∞/h_0, is much greater than 1. As a result, the swelling kinetics by the linear theory deviates from the nonlinear theory beyond the early stage. Apparently, the linear theory is applicable only for relatively small swelling ratios from the initial state. The same conclusion can be drawn for the kinetics of free swelling.

5.3. Comparison with experiments

Recently, Yoon *et al.*[11] reported measurements of swelling kinetics of thin poly(*N*-isopropylacrylamide) (PNIPAM) hydrogel layers under both constrained and freestanding conditions. Remarkably, they found that the measured swelling kinetics compared closely with the predictions based on the theory of linear poroelasticity, despite the fact that the relative swelling ratio (h_∞/h_0) was up to 1.8, which is apparently beyond the linear regime by the assumption of small deformation. The excellent agreement could be a fortuitous result of the fitting procedure. First, the Poisson's ratio was determined by comparing the measured thickness change at equilibrium for constrained swelling with that for free swelling. By linear poroelasticity, the ratio between the two equilibrium thickness changes, as given in (4.9) and (4.19), depends only on Poisson's ratio. However, as shown in Fig. 7, the linear poroelasticity theory underestimates the equilibrium swelling ratio in comparison with the nonlinear theory, especially for the cases with relatively large swelling ratios ($h_\infty/h_0 > 1.05$). By the nonlinear theory, the equilibrium swelling ratios, which can be determined from (4.3) and (4.15) respectively for the constrained and free swelling, depend on the intrinsic properties of the gel (χ and $N\Omega$) as well as the initial swelling ratio (λ_0). The ratio between the two equilibrium thickness changes, $\Delta^c_\infty/\Delta^f_\infty$, is plotted in Fig. 8 as a function of λ_0 for $N\Omega = 0.001$ and different values of χ. The predictions by the linear and the nonlinear theories agree only when the initial swelling ratio is close to the equilibrium free swelling ratio ($\lambda_0 \approx \lambda^f_\infty$). With the measured ratio $\Delta^c_\infty/\Delta^f_\infty = 2$, we cannot determine the three parameters (λ_0, χ and $N\Omega$) in the nonlinear theory.

Next, the effective diffusivity (D^*) in the linear poroelasticity theory was determined by fitting the self-similar solution in (4.10) to the data for constrained swelling at the early stage.[11] This is plausible since the linear theory is expected to be applicable at the early stage of swelling. With the self-similar kinetics at the early stage and the measured equilibrium thickness ratio ($\Delta^c_\infty/h_0 = 0.80$), the kinetics of constrained swelling was well described by the linear theory, despite the relatively large degree of swelling. With the same set of linear poroelastic parameters (ν, D^*, and Δ^c_∞/h_0), the kinetics of free swelling as predicted by the linear theory was also found to be in good agreement with the experiment. However, it is cautioned that the results should be interpreted within the fundamental limits of linear poroelasticity.

Here we suggest an alternative procedure to fit the experimental data using the nonlinear theory, which is applicable for large swelling ratios. To fully describe the swelling kinetics for both constrained and freestanding hydrogel layers, four parameters are to be determined: λ_0, χ, $N\Omega$, and D. In addition to the measurement of swelling kinetics, Yoon *et al.*[11] performed independent measurements of the shear modulus of the same gel by shear rheology. In principle, by measuring the shear modulus of the gel in the unswelled state (just after polymerization) and in the equilibrium state after free swelling, we obtain by (3.8): $G_0 = Nk_BT/\lambda_0$ and $G_\infty = Nk_BT/\lambda^f_\infty$. The measured values for the PNIPAM gel were: $G_0 = 1.3$ kPa and $G_\infty = 0.5$ kPa.[11] However, the ratio between the two moduli, $G_0/G_\infty = 2.6$, does not agree with the ratio, $\lambda^f_\infty/\lambda_0 = 1.4$, as measured from the free swelling experiment.[11] The discrepancy raises questions regarding the nonlinear theory as well as experimental uncertainties. Nevertheless, to illustrate the procedure of data fitting, we take one of the measured shear moduli (*e.g.*, $G_0 = 1.3$ kPa) and disregard the other. The three parameters, λ_0, χ, and $N\Omega$, can then be determined from the three measurable quantities, G_0, $R_c = h^c_\infty/h_0$, and $R_f = h^f_\infty/h_0$, by solving the following three equations simultaneously:

$$\frac{N\Omega}{\lambda_0} = \frac{\Omega G_0}{k_B T} \tag{5.3}$$

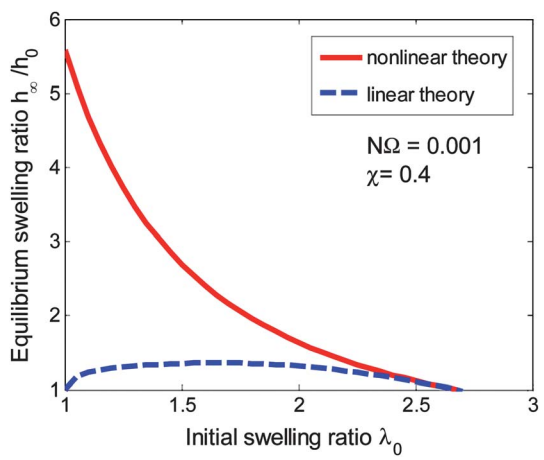

Fig. 7 Comparison of the equilibrium swelling ratio for a constrained hydrogel layer ($N\Omega = 0.001$ and $\chi = 0.4$), as predicted by the nonlinear theory and the linear poroelasticity.

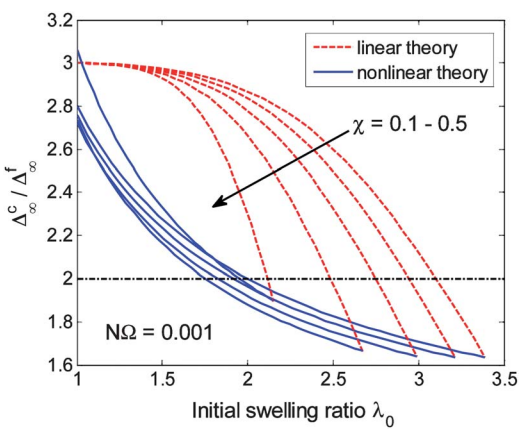

Fig. 8 The ratio between the equilibrium thickness changes for constrained and free swelling, predicted by the nonlinear theory as a function of the initial swelling ratio for $N\Omega = 0.001$ and $\chi = 0.1$–0.5, in comparison with the prediction by the linear poroelasticity theory (dashed lines).

$$\ln\left(1-\frac{1}{R_c\lambda_0^3}\right)+\frac{1}{R_c\lambda_0^3}+\frac{\chi}{R_c^2\lambda_0^6}+N\Omega\left(\frac{R_c}{\lambda_0}-\frac{1}{R_c\lambda_0^3}\right)=0 \quad (5.4)$$

$$\ln\left(1-\frac{1}{R_f^3\lambda_0^3}\right)+\frac{1}{R_f^3\lambda_0^3}+\frac{\chi}{R_f^6\lambda_0^6}+N\Omega\left(\frac{1}{R_f\lambda_0}-\frac{1}{R_f^3\lambda_0^3}\right)=0 \quad (5.5)$$

Using the measured values from Yoon *et al.*,[11] $G_0 = 1.3$ kPa, $R_c = 1.8$ and $R_f = 1.4$, along with $\Omega = 10^{-28}$ m^3 and $T = 298$ K, we obtain $\lambda_0 = 2.474$, $\chi = 0.4724$, and $N\Omega = 7.821 \times 10^{-5}$. The corresponding Poisson's ratio at the initial state is $\nu = 0.47$ by definition in (3.9). Using the same parameters, the Poisson's ratio at the fully swollen state is $\nu = 0.27$, which compares closely with reported values for PNIPAM gels from various measurements.[40,41] As noted in Fig. 5a, Poisson's ratio may change considerably from the initial state to the equilibrium state.

To determine the diffusivity (D), we compare the self-similar solution in (4.7) with the data for constrained swelling at the early stage. Using the effective diffusivity $D^* = 1.5 \times 10^{-11}$ m^2 s^{-1} obtained by Yoon *et al.*,[11] we obtain that

$$D = \frac{D^*}{\xi(\lambda_0^*)} = 1.098 \times 10^{-7} \text{ m}^2 \text{ s}^{-1} \quad (5.6)$$

Here $\lambda_0^* = (\lambda_0 + \lambda_\infty^c)/2 = 3.464$ has been used to account for instantaneous swelling near the surface as discussed in Section 4. On the other hand, by (3.17) and (3.12), the diffusivity can also be obtained as

$$D = D^*\frac{(1-2\nu)k_BT}{2(1-\nu)\Omega G_0}\frac{\lambda_0^3}{\lambda_0^3-1} = 2.74 \times 10^{-8} \text{ m}^2 \text{ s}^{-1} \quad (5.7)$$

which however underestimates the swelling rate. Since the surface of the hydrogel layer swells instantaneously to a large degree ($\lambda_\infty^c/\lambda_0 = 1.8$), the linear theory with all properties defined at the initial state cannot correctly predict the swelling kinetics near the surface even at the early stage.

With all the parameters determined from (5.3) to (5.6), Fig. 9 compares the swelling kinetics by the nonlinear theory with the linear theory. Using the parameters determined by Yoon *et al.*,[11] the linear theory agrees closely with the experimental data. Thus, Fig. 9 can be considered as a comparison between the nonlinear theory and the experiment. As expected from the data fitting procedure, the nonlinear theory reproduces the two equilibrium swelling ratios and the kinetics of constrained swelling at the early stage. The kinetics of free swelling at the early stage, not used for data fitting, is correctly predicted by the nonlinear theory.[50] However, relatively large discrepancy is notable beyond the early stage, although it is comparable to the scattering of the experimental data.

5.4. The indentation method

Indentation experiments have been demonstrated recently as an effective method for characterizing poroelastic properties of gels.[8–15] By imposing relatively shallow indentation displacements into a saturated gel and measuring force relaxation as a function of time, the linear poroelastic properties can be fully determined without ambiguity. Such a method is efficient from both experimental and theoretical points of view. The procedure of the indentation experiment is relatively simple, and the analysis of the data is fairly straightforward within the theoretical framework of linear poroelasticity due to small deformation. As shown by Hu *et al.*,[12] the measured elastic constants (G and ν) can be interpreted within the Flory–Huggins theory for nonlinear analysis. Since the gel is fully saturated with the solvent, the swelling ratio λ_0 is determined by the intrinsic properties (χ and $N\Omega$) of the gel as given in eqn (3.1) with $\mu_0 = 0$. Thus the elastic constants measured by the indentation method are the linear properties at the vicinity of the fully swollen state of the gel. Furthermore, the effective diffusivity (D^*) measured by the indentation method can be converted to the intrinsic diffusivity D in the nonlinear theory, as given in (5.7). Therefore, all the intrinsic properties in the nonlinear theory can be determined from the indentation method, which would then enable prediction of the nonlinear behaviour of the gel with large deformation. In particular, a comparison between a full nonlinear analysis of the force relaxation during indentation and the linear poroelasticity solution would be useful to quantitatively define the shallow indentation requirement for the linear analysis.

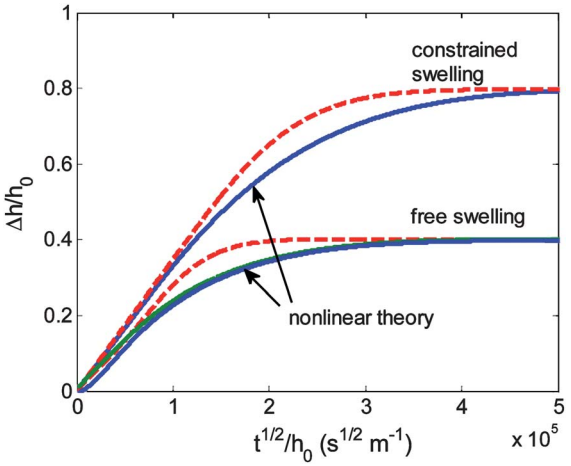

Fig. 9 A comparison between the nonlinear theory and experimental results for kinetics of constrained and free swelling. The dashed lines reproduce the predictions of linear poroelasticity using the parameters determined by Yoon *et al.*[11] to fit their experimental data. The solid lines are numerical results based on the nonlinear theory using the parameters determined from (5.3) to (5.6): $\lambda_0 = 2.474$, $\chi = 0.4724$, $N\Omega = 7.821 \times 10^{-5}$, and $D = 1.098 \times 10^{-7}$ m^2 s^{-1}.

As noted by Hui *et al.*,[8] it is possible to extend the analysis of the indentation experiment to include the effect of adhesion. Polymer gels are often sensitive to adhesive interactions with other materials coming into contact. Contact mechanics with the effect of adhesion has been developed and widely used to characterize adhesive interactions between surfaces.[42,43] However, most studies have assumed elastic behavior of the interacting solids, and extension to poroelastic solids would be desirable for the study of adhesion between polymer gels. In addition, many applications use gels in the form of thin layers.[13] Constrained swelling of thin layers results in an anisotropic swollen state.[33] Indentation upon such a gel layer should be analyzed using an anisotropic poroelasticity theory. The linearization procedure in Section 3 of the present work can be easily extended to develop a set of linear equations for anisotropic poroelasticity consistent with the nonlinear theory. Then the anisotropic poroelastic

contact problem may be solved by extending the solution to the corresponding elastic contact problem for anisotropic materials.[44,45] Further extension of the indentation method may be developed to characterize polymer gels in the form of patterned lines and particles.[46–49] The analysis would be necessarily complicated due to the geometry and likely inhomogeneous swelling. Numerical analysis based on the nonlinear theory would be required along with experimental measurements, which may be used to probe the effects of size and shape on the mechanical and transport properties of polymer gels.

6. Conclusion

In summary, we present a comparison between a nonlinear theory for polymer gels and the classical theory of linear poroelasticity. We show that the two theories are consistent within the linear regime under the condition of small perturbation from an isotropically swollen state of the gel. The relationship between the material properties in the linear theory and those in the nonlinear theory is established by a linearization procedure. Both linear and nonlinear solutions are presented for swelling kinetics of substrate-constrained and freestanding hydrogel layers. Although the linear poroelasticity theory can be used to fit the experimental data, it is cautioned that the applicability of the linear theory should be limited to relatively small swelling ratios. For large swelling ratios, a new procedure is suggested to fit the experimental data with the nonlinear theory. Finally, we discuss the indentation experiment as an effective method for characterizing the mechanical and transport properties of polymer gels in the linear regime along with possible extensions of the method.

Acknowledgements

The authors gratefully acknowledge financial support by National Science Foundation (grant no. 0926851).

Notes and references

1 T. Tanaka, L. Hocker and G. Benedek, *J. Chem. Phys.*, 1973, **59**, 5151.
2 T. Tanaka and D. Fillmore, *J. Chem. Phys.*, 1979, **70**, 1214.
3 G. W. Scherer, *J. Non-Cryst. Solids*, 1989, **113**, 107.
4 G. W. Scherer, *J. Non-Cryst. Solids*, 1992, **144**, 210.
5 M. A. Biot, *J. Appl. Phys.*, 1941, **12**, 155.
6 D. L. Johnson, *J. Chem. Phys.*, 1982, **77**, 1531.
7 C.-Y. Hui and V. Muralidharan, *J. Chem. Phys.*, 2005, **123**, 154905.
8 C.-Y. Hui, Y. Y. Lin, F.-C. Chuang, K. R. Shull and W.-H. Lin, *J. Polym. Sci., Part B: Polym. Phys.*, 2006, **43**, 359.
9 M. Galli, K. S. C. Comley, T. A. V. Shean and M. L. Oyen, *J. Mater. Res.*, 2009, **24**, 973.
10 Y. Hu, X. Zhao, J. J. Vlassak and Z. Suo, *Appl. Phys. Lett.*, 2010, **96**, 121904.
11 J. Yoon, S. Cai, Z. Suo and R. C. Hayward, *Soft Matter*, 2010, **6**, 6004.
12 Y. Hu, X. Chen, G. M. Whitesides, J. J. Vlassak and Z. Suo, *J. Mater. Res.*, 2011, **26**, 785.
13 Y. Hu, E. P. Chan, J. J. Vlassak and Z. Suo, *J. Appl. Phys.*, 2011, **110**, 086103.
14 E. P. Chan, Y. Hu, P. M. Johnson, Z. Suo and C. M. Stafford, *Soft Matter*, 2012, **8**, 1492.
15 Z. I. Kalcioglu, R. Mahmoodian, Y. Hu, Z. Suo and K. J. Van Vliet, *Soft Matter*, 2012, **8**, 3393.
16 C. Durning and K. Morman Jr, *J. Chem. Phys.*, 1993, **98**, 4275.
17 B. Barriere and L. Leibler, *J. Polym. Sci., Part B: Polym. Phys.*, 2003, **41**, 166.
18 K. Rajagopal, *Mater. Sci. Technol.*, 2003, **19**, 1175.
19 S. Baek and A. Srinivasa, *Int. J. Nonlinear Mech.*, 2004, **39**, 201.
20 J. E. Dolbow, E. Fried and H. Ji, *J. Mech. Phys. Solids*, 2004, **52**, 51.
21 H. Ji, H. Mourad, E. Fried and J. E. Dolbow, *Int. J. Solids Struct.*, 2006, **43**, 1878.
22 E. Birgersson, H. Li and S. Wu, *J. Mech. Phys. Solids*, 2008, **56**, 444.
23 W. Hong, X. Zhao, J. Zhou and Z. Suo, *J. Mech. Phys. Solids*, 2008, **56**, 1779.
24 F. Duda, A. Souza and E. Fried, *J. Mech. Phys. Solids*, 2010, **58**, 515.
25 S. A. Chester and L. Anand, *J. Mech. Phys. Solids*, 2010, **58**, 1879.
26 P. J. Flory and J. Rehner, *J. Chem. Phys.*, 1943, **11**, 521.
27 P. J. Flory, *Principles of Polymer Chemistry*, Cornell University Press, Ithaca, NY, 1953.
28 T. Tanaka, S. T. Sun, Y. Hirokawa, S. Katayama, J. Kucera, Y. Hirose and T. Amiya, *Nature*, 1987, **325**, 796.
29 V. Trujillo, J. Kim and R. C. Hayward, *Soft Matter*, 2008, **4**, 564.
30 A. Peter and S. J. Candau, *Macromolecules*, 1986, **19**, 1952.
31 M. Doi, *J. Phys. Soc. Jpn.*, 2009, **78**, 052001.
32 Y. Li and T. Tanaka, *J. Chem. Phys.*, 1990, **92**, 1365.
33 M. K. Kang and R. Huang, *J. Appl. Mech.*, 2010, **77**, 061004.
34 M. A. Biot, *J. Appl. Phys.*, 1955, **26**, 182.
35 M. M. Carroll, *J. Geophys. Res.*, 1979, **84**, 7510.
36 M. Thompson and J. R. Willis, *J. Appl. Mech.*, 1991, **58**, 612.
37 A. H.-D. Cheng, *Int. J. Rock Mech. Mining Sci.*, 1997, **34**, 199.
38 S. C. Cowin, *J. Biomech.*, 1999, **32**, 217.
39 S. S. Kohles and J. B. Roberts, *J. Biomech. Eng.*, 2002, **124**, 521.
40 S. Hirotsu, *J. Chem. Phys.*, 1991, **94**, 3949.
41 C. Li, Z. Hu and Y. Li, *Phys. Rev. E: Stat. Phys., Plasmas, Fluids, Relat. Interdiscip. Top.*, 1993, **48**, 603.
42 K. L. Johnson, K. Kendall and A. D. Roberts, *Proc. R. Soc. London, Ser. A*, 1971, **324**, 301.
43 M. K. Chaudhury and G. M. Whitesides, *Langmuir*, 1991, **7**, 1013.
44 J. R. Willis, *J. Mech. Phys. Solids*, 1966, **14**, 163.
45 J. J. Vlassak and W. D. Nix, *J. Mech. Phys. Solids*, 1994, **42**, 1223.
46 V. Tirumala, R. Divan, L. Ocola and D. Mancini, *J. Vac. Sci. Technol., B*, 2005, **23**, 3124.
47 S. J. DuPont Jr, R. S. Cates, P. G. Stroot and R. Toomey, *Soft Matter*, 2010, **6**, 3876.
48 M. K. Kang and R. Huang, *Int. J. Appl. Mech.*, 2011, **3**, 219.
49 M. Caldorera-Moore, M. K. Kang, Z. Moore, V. Singh, S. V. Sreenivasan, L. Shi, R. Huang and K. Roy, *Soft Matter*, 2011, **7**, 2879.
50 In Fig. 9, two curves are plotted for free swelling according to the nonlinear theory, one for the average thickness ratio ($\Delta h/h_0$) and the other for in-plane swelling ratio ($\lambda_1/\lambda_0 - 1$). The two curves are slightly different at the early stage of swelling as shown more clearly in Fig. 4b. The curve for in-plane swelling ratio agrees more closely with the experimental data, which was actually obtained by measuring the in-plane swelling instead of the thickness ratio [11].